



Evaluation of the Fidelity of Additively Manufactured 3D Models of a Fossil Skull

Mirosław Rucki¹ (✉), Yaroslav Garashchenko², Ilja Kogan^{3,4}, and Tomasz Ryba⁵

¹ Faculty of Mechanical Engineering, Kazimierz Pulaski University of Technology and Humanities in Radom, ul. Stasieckiego 54, 26-600 Radom, Poland
m.rucki@uthrad.pl

² Department of Integrated Technologic Process and Manufacturing, National Technical University «Kharkiv Polytechnic Institute», Kyrpychova Street 2, Kharkiv 61002, Ukraine

³ TU Bergakademie Freiberg, Geological Institute, Bernhard-von-Cotta-Street 2, 09599 Freiberg, Germany

⁴ Institute of Geology and Petroleum Technologies, Kazan Federal University, Kremlyovskaya 4/5, 420008 Kazan, Russia

⁵ Sieć Badawcza Łukasiewicz, Instytut Technologii Eksploatacji w Radomiu, ul. K. Pułaskiego 6/10, 26-600 Radom, Poland

Abstract. The paper presents a comparative analysis of the 3D-printed models of a complex geometrical object obtained using different Additive Manufacturing technologies. The object of interest is a unique fossil skull of a ‘reptiliomorph amphibian’ *Madygenerpeton pustulatum*. Twelve different copies were 3D-printed using the same (reference) digitized model and then scanned with a Mitutoyo Coordinate Measuring Machine (CMM) CRYSTA-Apex S 9166. Fidelity of each copy was assessed through the comparison with the reference digital model and with each other in couples. Statistical analysis of the distances between compared surfaces provided good background for the choice of the most accurate copies.

Keywords: Additive manufacturing · *Madygenerpeton* · Optical measurement

1 Introduction

Additive manufacturing (AM) technologies are relatively new methods using an incremental layer-by-layer materialization of a digital model. The AM methods referred to also as 3D printing (3DP), rapid prototyping (RP), or solid-freeform (SFF) became an exponentially evolving manufacturing technology [1]. The estimated average global value of the 3D printing market is recording a 25% year-to-year increase since 2014, and is expected to reach 35.0 billion USD by 2024 [2]. A good review of these methods can be found in [3], as well as in more recent works related to Industry 4.0 and Internet of Things concepts [4, 5]. It is emphasized that the cost of Additive Manufacturing is a crucial factor [6]. There are also works that discuss design principles, constrains and optimization for AM techniques [7].

At present, a large variety of individual additive processes are available depending on a material and machine technology, which can be classified into the seven main categories: material jetting, binder jetting, vat photopolymerization, material extrusion, powder bed fusion, sheet lamination, and direct energy deposition [8]. AM allows for hybrid- and multi-material (MM) manufacturing of metals and is especially suitable for functionally graded materials (FGMs) [9]. There are well-established and rapidly emerging applications of AM technologies, such as rapid fabrication of a prototype, micro-scale manufacturing for aerospace and motor industries, medical applications, rapid tooling, direct digital manufacturing, as well as an increasing number of new applications far beyond the initial intent of prototyping [10].

From the literature review it can be concluded that among the main directions of 3D-printing development are geometry and material design for AM, computational tools and interfaces development, as well as manufacturing tools and processes development [11]. In most of published research papers, attention is paid to the optimization tasks of AM-process planning [12], CAD-AM (RP) programs [13], choice of AM technologies [14], the synthesis principles applied during the manufacturing process [15], design of cladding layers, the proper choice of building materials, as well as finally obtained surface quality [16], dimensional accuracy [17], as well as microstructures and properties [18]. The objective of this paper is to assess fidelity of the 3D-printed models of a natural complex geometrical object with no initial documentation, fabricated using different Additive Manufacturing technologies. The object of interest is a fossil skull of a 'reptiliomorph amphibian' *Madygenerpeton pustulatum* [19] from the Triassic of Kyrgyzstan. The skull is somewhat deformed and lacking the lower jaw, but because of its uniqueness it is of great interest to the paleontological community, and its 3D-printed models are intended for exhibitions, teaching and research purposes.

2 Materials and Methods

The replicated object is the holotype of *Madygenerpeton pustulatum* [19], an incomplete fossil skull that was recovered in 2007 from the fossil deposit Madygen in southwest Kyrgyzstan [20], world's arguably richest non-marine finding locality of Triassic fossils (ca. 237 million years before present). This unique skull has been deformed by fossilization processes and lacks the lower jaw. Figure 1 presents the overall view of the fossil and the close-up image of its surface morphology with bony tubercles covering the skull. No complete remains of *Madygenerpeton pustulatum* individual has been found. Bony carapace shields (osteoderms) discovered next to the skull belonged to at least three individuals of the same species. *Madygenerpeton* is a member of the extinct *Chroniosuchia*, a group of derived amphibians close to the origin of all higher vertebrates (mammals and reptiles including birds), and is reconstructed to have been a crocodile-like predatory animal adapted to both terrestrial and aquatic locomotion. It can be assumed that the osteoderms would act as an additional trunk support while walking on land, but at the same time, their weight would push the body below the water surface when dwelling in water [21].

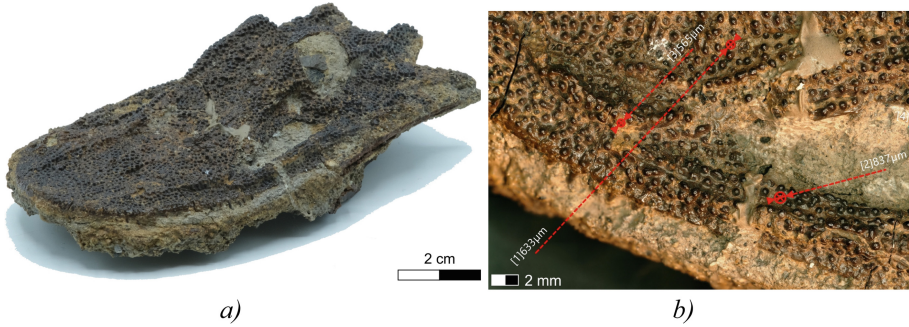


Fig. 1. Fossil skull of *Madygenerpeton pustulatum* (holotype FG 596/V/4, housed at the TU Bergakademie Freiberg): a) view, and b) close-up picture of surface morphology.

To reach the main objective of the research, following steps were undertaken:

- Preparation of the 3D-printed copies of the object using the same digital model (later used as a reference), but different AM techniques,
- Scanning of the physical copies of the object to obtain their digital models,
- Visual and statistical analysis of the differences between the initial (reference) digital model,
- Detailed statistical analysis of the differences in order to determine peculiarities of the applied AM methods and to point out the most suitable one for the investigated *Madygenerpeton* fossil skull.

After scanning of the object with different scanning techniques, rating of the digital models was made [22]. In the rating, the digitization with AICON SmartScan exhibited the lowest distances to the models obtained from other scanners. Nevertheless, for the 3D-printing of the copies, Artec Space Spider digitized model was chosen. It was in the third place of the rating, which can be considered as proof for high accuracy. Moreover, it was advantageous for practical reasons, namely, it provided better the detailed geometry of the smallest elements of the fossil skull. As a result, the digitized ‘Artec surface model’ was $20,978.512 \text{ mm}^2$, which was by 11.8% larger than that obtained from AICON device. Thus, the reference digital surface in this research was the model obtained from scanning the fossil skull with the Artec Space Spider device.

Next, 12 physical copies of the object were 3D-printed using a wide range of the available AM techniques. Table 1 shows the main data of the devices and parameters used in experiments, while the Fig. 2 presents the photo of model #7 made out of the apricot kernel flour.

The 3D-printed copies were then scanned with a Mitutoyo Coordinate Measuring Machine (CMM) CRYSTA-Apex S 9166 at Mitutoyo Polska, Wrocław. The maximum permissible error of the CMM was $MPE_E = \pm (1.7 + 3L/1000) \mu\text{m}$. The surface scanning was performed with non-contact line laser probe SurfaceMeasure 606 with scanning error $12 \mu\text{m}$ [1σ / sphere fit]. Its accuracy was found satisfactory after preliminary analysis [23]. The scanning procedure was performed in a single fixation in order to minimize the error generated by the formation of a points cloud.

Table 1. Technologies and devices used for manufacture of the fossil skull copies.

Copy No	Technologies	Equipment model	Material	Layer thickness, mm
#1	Extrusion-based FDM	Ultimaker 2 +	PLA	0.100
#2	Multijet fusion	HP jet fusion 3D 4210	Polyamid PA 12-HP	0.080
#3	Extrusion-based FDM	Prusa i3 MK2	PLA	0.050
#4	Powder-based 3D printing with inkjet	Canon ProJet 460Plus	White gypsum	0.125
#5	UV-resin-Inkjet	Continuous inkjet printers keyence	Yellowish transparent	0.100
#6	Powder-based 3D printing with inkjet	ZCorp 310(R)	Gypsum, ZP151	0.088
#7	Powder-based 3D printing with inkjet	ZCorp 310(R)	Apricot kernel flour	0.088
#8	Polyjet	Stratasys J55	Standard material	0.019
#9	Polyjet	Stratasys J55	Vivid material	0.019
#10	ColorJet printing	3D Systems ProJet CJP 460Plus	VisiJet PXL	0.100
#11	ColorJet printing	3D systems Zprinter 650	VisiJet PXL	0.089
#12	UV-curable inkjet printing	Mimaki 3DUJ-553	SW-100	0.032

**Fig. 2.** Example of the 3D printed model, #7 made out of apricot kernel flour.

The comparative analysis of the 3D-printed copies fidelity was performed using Δs distances between the reference ‘Artec surface model’ and each of the surfaces obtained from the scanning of the respective physical copies. For the analysis, the system Geomagic Studio was used. Initial comparison consisted of minimization of the distances between two digital surfaces based on 2000 points. Further, detailed statistical analysis of the preliminary data was performed using CAD system PowerShape and Statistica software.

3 Results and Discussion

Analysis of Δs distances between the reference model and the respective scanned surfaces was somewhat limited by the application of a single fixation during the scanning of copies. As a result, the measuring points were collected from the upper side of the object only. The reference model, in turn, was a closed 3D surface, since the scanning procedure was performed from sides and the top with a further connection of the obtained points to one digital model. It caused somewhat overestimated values of Δs in some areas of the surface. In order to minimize overestimation, maximal distance between two compared surfaces was limited down to 5 mm. This limitation excluded from the statistical calculations some 24.7% of the surface at average, with maximal and minimal percentage 58% and 12%, respectively.

3.1 Results of Preliminary Comparison

The results of comparison between the reference digital surface and each of the scanned models were presented visually in form of a colored deviation map. Calculated maximal values of Δs distances above and below the reference surface were denoted as positive and negative, respectively. The average, apart from the overall one, was calculated additionally for negative and positive values. These results are shown in Table 2.

Table 2. Calculated distances Δs (mm) between the reference digital surface and scanned copies.

Copy no.	Maximum		Average			Standard deviation
	Positive	Negative	Overall	Positive	Negative	
#1	1.443	-1.894	-0.012	0.259	-0.193	0.273
#2	5.000	-2.272	0.044	0.165	-0.082	0.349
#3	2.445	-4.673	-0.015	0.069	-0.088	0.151
#4	2.494	-3.923	-0.053	0.093	-0.130	0.189
#5	-	-	-	-	-	-
#6	1.529	-2.240	-0.016	0.085	-0.096	0.116
#7	2.891	-3.675	-0.031	0.251	-0.232	0.299
#8	0.748	-2.860	-0.002	0.057	-0.061	0.075
#9	0.564	-0.696	-0.009	0.065	-0.073	0.086
#10	1.196	-2.971	-0.016	0.070	-0.078	0.094
#11	2.025	-3.570	-0.012	0.054	-0.067	0.089
#12	1.577	-3.637	-0.010	0.071	-0.088	0.105

Figures 3 and 4 present examples of the colored maps of Δs distances between the reference digital surface and scanned surfaces of copies #1 and #9, respectively. Large values of Δs distances above ± 1 mm are seen in Fig. 3, while only minor areas lay more than 0.2 mm above or below the reference surface.

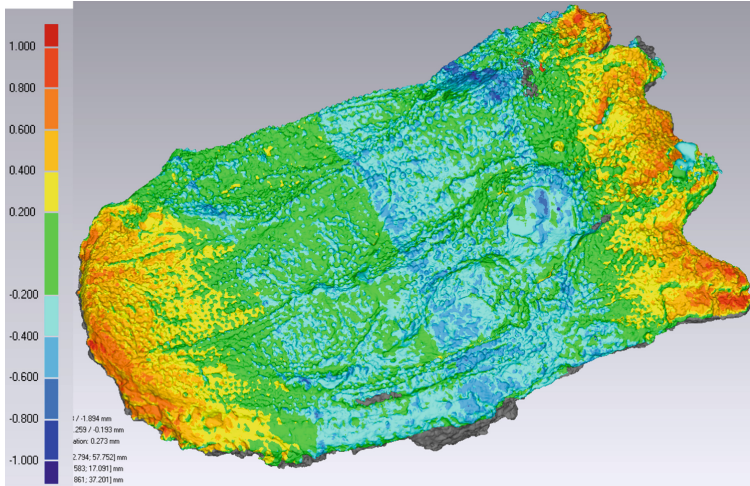


Fig. 3. Example of the colored map of Δs distances between reference digital surface and scanning results of copy #1.

From the visual analysis of the collected colored maps of deviations, copies #1, #4, #6, and #7 were found the most inaccurate. Especially copy #1 shown in Fig. 3 exhibited large areas inaccurately represented by the 3D-printing process.

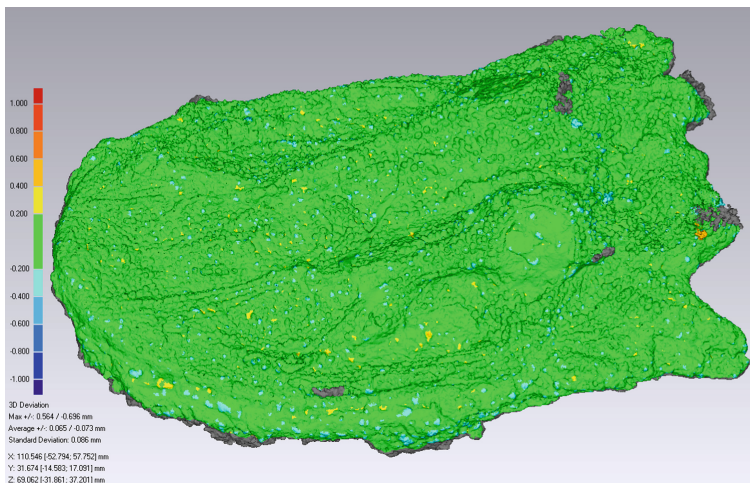


Fig. 4. Δs deviations between reference digital surface and scanning results of copy #9.

Based on the average distances from the reference model, it was found useful to plot a graph of the obtained standard deviations versus average distances. This is presented in Fig. 5.

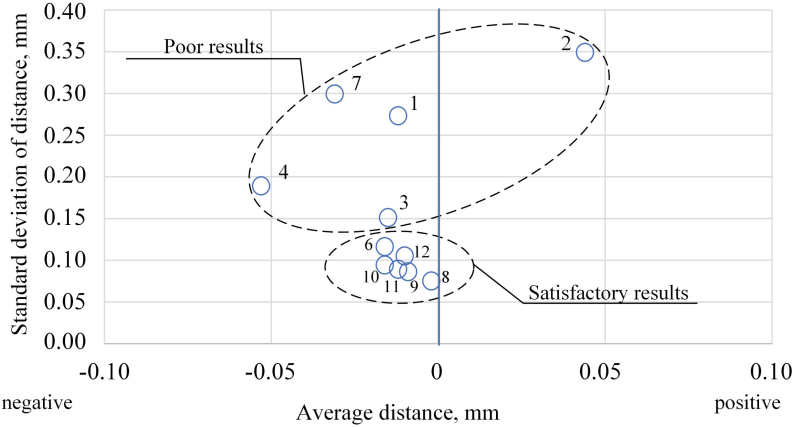


Fig. 5. Graphical analysis of the accuracy of scanned models based on distances Δs .

Model #2 exhibits the largest standard deviation combined with the largest average distance from the reference surface, hence, it can be considered the less accurate representation of the object. On the other hand, model #8 shows the smallest respective values, and as such it could be considered the most accurate one. However, because of small standard deviations close to 0.10 mm, some other models can be considered satisfactory and undergo further detailed analysis. The ones grouped as ‘poor results’ may be recommended against the use for 3D-printing of the analyzed fossil skull.

3.2 Statistical Analysis of the Results

Further statistical analysis of the obtained data was carried out using CAD system PowerShape. Due to the fact, that in different CAD systems different algorithms can be applied for calculations of the distances between digital surfaces, this approach provides reasonable ground for evaluation of the fidelity of the fossil skull copies.

Figure 6 presents graphically the results of the analysis of Δs distances distribution by means of the ‘Box Whiskers’ diagrams. The boxplot of multiple variables does not contain outliers and extremes because they bear no useful information. Their real values apparently do not fit the algorithm. Results in Fig. 6 allow for including copies #3 and #6 to the group of satisfactory results. In fact, this analysis demonstrates the complexity of the issue, so that decision on the feasibility of an AM method should not be based on a single parameter.

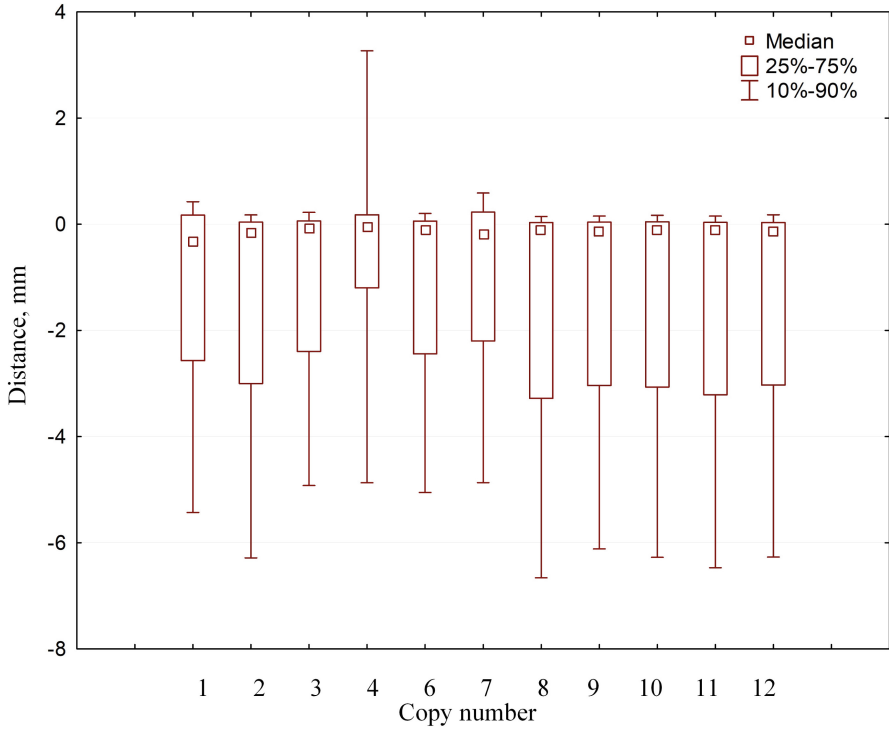


Fig. 6. Results of the statistical analysis of distances between the reference surface and scanned copies.

Thus, one more comparative analysis was performed. Namely, the scanned surfaces of the 3D-printed copies were compared to each other in couples in order to point out the surfaces closest to each other. Graphical presentation of the obtained standard deviations versus average distances between surfaces of each two copies is shown in Fig. 7.

Based on the results from Fig. 7, it was possible to arrange the copies in the rating list. The main criterion was the square root distance $\sigma\{\Delta s\}$ between the digitized surfaces of the respective copies. First, each couple was ascribed a number according to the value of $\sigma\{\Delta s\}$, and then the sum of these numbers determined the rating of each model. As a result, the copies were put in the following row from the closest one down to the one most distanced from others: #11 \rightarrow #12 \rightarrow #9 \rightarrow #6 \rightarrow #10 \rightarrow #3 \rightarrow #8 \rightarrow #4 \rightarrow #7 \rightarrow #1.

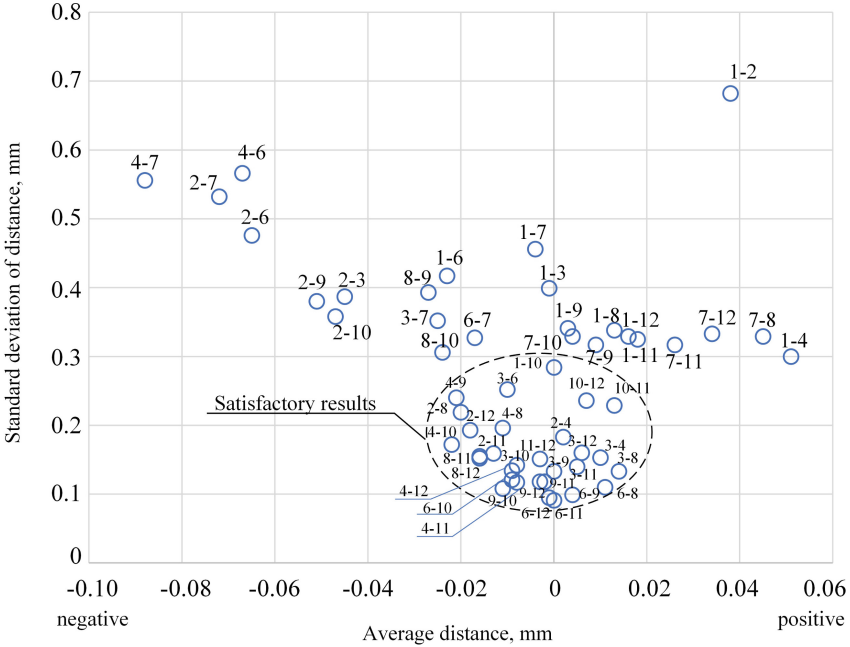


Fig. 7. Standard deviations versus average distances between the reference surface and scanned copies.

3.3 Detailed Statistics for Chosen Copies

From the abovementioned rating list, four of the first copies were chosen for the detailed statistical analysis using the Statistica software. Distances Δs between the reference digital surface and each scanned copy were taken from the results obtained from Autodesk PowerShape analysis. Figure 8 presents histograms and main statistical characteristics of the respective copies.

It is noteworthy that the obtained histograms are quite similar to one another, except for copy #6 that exhibits slightly different distribution of the distances Δs . For the square root distance $\sigma\{\Delta s\}$, for copies #6, #9, #12, and #11 the dispersion is rather narrow, from 0.0134 to 0.0159 mm. At the same time, median $Me\{\Delta s\}$ changes between -0.128 and -0.0979 mm, which can be considered a narrow range. These results confirm that the printed copies are close to each other in terms of surface reproduction fidelity.

Hence, all these four methods can be recommended as feasible for additive manufacture of the copies of a fossil skull similar to that of *Madygenerpeton* with an accuracy of ± 0.4 mm over the most of its surface. Reference to the abovementioned rating can be helpful, and other factors can be considered, such as price, availability, time, etc.

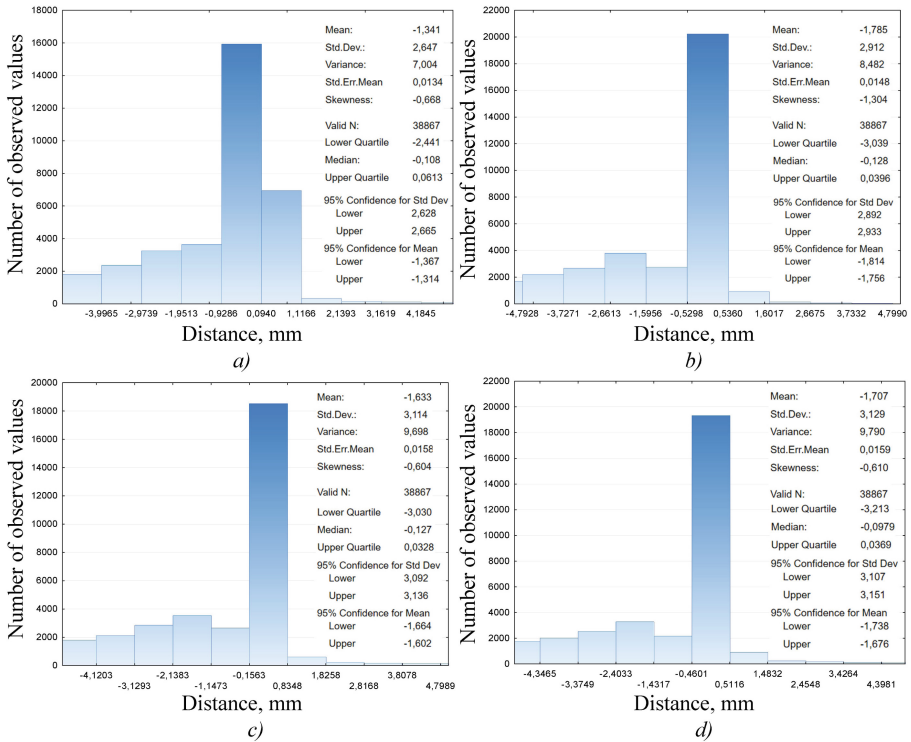


Fig. 8. Statistical parameters and histograms of distribution of distances Δs between the reference surface and scanned copies: a) #6, b) #9, c) #12, d) #11.

It can be presumed that a more accurate scanning method would provide better digital surfaces for the comparative analysis and, hence, would give more unequivocal recommendations. However, the optical surface properties of different copies, related to the surface texture, material characteristics, etc., make it impossible to find a single scanning method of the highest accuracy for all the printed copies.

Further research will cover a wider spectrum of the AM technologies able to produce reasonably accurate copies of the *Madygenperpeton* fossil skull. Additionally, it is interesting to consider different methods of scanning in order to find statistical background for comparison of the accuracy of the 3D-printed objects.

4 Conclusions

From the performed analysis of Δs distances between the reference model and the respective scanned surfaces of 3D-printed copies of *Madygenperpeton* fossil skull, the following conclusions can be derived.

First of all, there are certain limitations of the evaluation of the copies' accuracy due to different optical properties of the surfaces obtained from different AM methods. The same scanning method may provide highly accurate results for one 3D-printed copy, but not so accurate for another.

Next, the analysis based on Δs distances and on the standard deviation of their distribution throughout the scanned surface provided reliable results. From this analysis, a group of the copies of poor fidelity was identified. Further detailed statistics proved that the models identified as satisfactory accurate had similar distribution histograms, and based on the criterion of the square root distance $\sigma\{\Delta s\}$ between the digitized surfaces, the rating list was created.

And finally, it was demonstrated, that the proposed methodology was helpful in evaluation of the fidelity of additively manufactured copies of such a unique object as a *Madygenerpeton* fossil skull. Similar methodology can be applied for any paleontological object or a unique artifact where some individual features have to be copied and reproduced with high fidelity.

Acknowledgements. Results presented in this paper were achieved in the frame of the ESF-funded young researcher group “G.O.D.S.” (Geoscientific Objects Digitization Standards) at the TU Bergakademie Freiberg. This paper has been supported by the Kazan Federal University Strategic Academic Leadership Program.

Authors express their gratitude to the colleagues who helped with the acquisition of 3D data, in particular Daniel Eger Passos and Sascha Schmidt (Freiberg), Maik Jähne, Henrik Alhers and Thomas Reuter (Dresden), Kristin Mahlow and Tom Cvjetkovic (Berlin), Tomasz Szymański and Robert Długoszewski (Mitutoyo Polska, Wrocław).

References

1. Zhang, X., Fan, W., Liu, T.: Fused deposition modeling 3D printing of polyamide-based composites and its applications. *Compos. Commun.* **21**, 100413 (2020)
2. Woźniak, J., Budzik, G., Przeszlowski, Ł., Chudy-Laskowska, K.: Directions of the development of the 3D printing industry as exemplified by the polish market. *Manag. Prod. Eng. Rev.* **12**(2), 98–106 (2021)
3. Gardan, J.: Additive manufacturing technologies: state of the art and trends. *Int. J. Prod. Res.* **54**(10), 3118–3132 (2016)
4. Elhoone, H., Zhang, T., Anwar, M., Desai, S.: Cyber-based design for additive manufacturing using artificial neural networks for Industry 4.0. *Int. J. Prod. Res.* **58**(9), 2841–2861 (2020)
5. Wang, Y., Lin, Y., Zhong, R.Y., Xu, X.: IoT-enabled cloud-based additive manufacturing platform to support rapid product development. *Int. J. Prod. Res.* **57**(12), 3975–3991 (2019)
6. Rosienkiewicz, M., Gabka, J., Helman, J., Kowalski, A., Susz, S.: Additive manufacturing technologies cost calculation as a crucial factor in industry 4.0. In: Hamrol A., Ciszak O., Legutko S., Jurczyk M. (eds.) *Advances in Manufacturing. Lecture Notes in Mechanical Engineering*, pp. 171–183. Springer, Cham (2018). https://doi.org/10.1007/978-3-319-68619-6_17
7. Tsirogiannis, E., Vosniakos, G.: Redesign and topology optimization of an industrial robot link for additive manufacturing. *Facta Univ. Ser. Mech. Eng.* **17**(3), 415–424 (2019)
8. Singh, R., et al.: Powder bed fusion process in additive manufacturing: an overview. In: *Materials Today: Proceedings 26 (Part 2)*, pp. 3058–3070 (2020)
9. Schneck, M., Horn, M., Schmitt, M., Seidel, C., Schlick, G., Reinhart, G.: Review on additive hybrid- and multi-material-manufacturing of metals by powder bed fusion: state of technology and development potential. *Prog. Addit. Manuf.* **6**(4), 881–894 (2021)
10. Gibson, I., Rosen, D., Stucker, B., Khorasani, M.: *Additive Manufacturing Technologies*. 3rd edn. Springer, Cham (2021). <https://doi.org/10.1007/978-3-030-56127-7>

11. Gao, W., et al.: The status, challenges, and future of additive manufacturing in engineering. *Comput. Aided Des.* **69**, 65–89 (2015)
12. Di Angelo, L., Di Stefano, P., Guardiani, E.: Search for the optimal build direction in additive manufacturing technologies: a review. *J. Manuf. Mater. Process.* **4**(3), 71 (2020)
13. Dalpadulo, E., Pini, F., Leali, F.: Assessment of design for additive manufacturing based on CAD platforms. In: Rizzi, C., Andrisano, A.O., Leali, F., Gherardini, F., Pini, F., Vergnano, A. (eds.) *ADM 2019. LNME*, pp. 970–981. Springer, Cham (2020). https://doi.org/10.1007/978-3-030-31154-4_83
14. Zhang, Y., Xu, Y., Bernard, A.: A new decision support method for the selection of RP process: knowledge value measuring. *Int. J. Comput. Integr. Manuf.* **27**(8), 747–758 (2014)
15. Razavykia, A., Brusa, E., Delprete, C., Yavari, R.: An overview of additive manufacturing technologies — a review to technical synthesis in numerical study of selective laser melting. *Materials* **13**(17), 3895 (2020)
16. Di Angelo, L., Di Stefano, P., Marzola, A.: Surface quality prediction in FDM additive manufacturing. *Int. J. Adv. Manuf. Technol.* **93**(9–12), 3655–3662 (2017)
17. Chen, H., Zhao, Y.F.: Process parameters optimization for improving surface quality and manufacturing accuracy of binder jetting additive manufacturing process. *Rapid Prototyping J.* **22**(3), 527–538 (2016)
18. Li, N., et al.: Progress in additive manufacturing on new materials: a review. *J. Mater. Sci. Technol.* **35**, 242–269 (2019)
19. Schoch, R.R., Voigt, S., Buchwitz, M.: A chroniosuchid from the Triassic of Kyrgyzstan and analysis of chroniosuchian relationships. *Zool. J. Linn. Soc.* **160**, 515–530 (2010)
20. Voigt, S., et al.: Triassic life in an inland lake basin of the warm-temperate biome – the Madygen Lagerstätte (southwest Kyrgyzstan, Central Asia). In: Fraser, N.C., Sues, H.D. (eds.) *Terrestrial conservation Lagerstätten. Windows into the evolution of life on land*, pp. 65–104. Dunedin, Edinburgh, London (2017)
21. Buchwitz, M., Witzmann, F., Voigt, S., Golubev, V.: Osteoderm microstructure indicates the presence of a crocodylian-like trunk bracing system in a group of armoured basal tetrapods. *Acta Zoologica* **93**(3), 260–280 (2012)
22. Garashchenko, Y., Kogan, I., Rucki, M. Analysis of 3D triangulated models of *Madygen-erpeton pustulatum* fossil skull. In: *Euspen's 21st International Conference & Exhibition*, pp. 89–90. Copenhagen, DK, June 2021
23. Kogan, I., Rucki, M., Jähne, M., Eger Passos, D., Cvjetkovic, T., Schmidt, S.: One head, many approaches – comparing 3D models of a fossil skull. In: Luhmann, T., Schumacher, C. (eds.), *Photogrammetrie – Laserscanning – Optische 3D-Messtechnik: Beiträge der Oldenburger 3D-Tage 2020*, pp. 22–31. Wichmann Verlag, Berlin (2020)